

Nickel limited methanogens shaped Precambrian climate

Heng Wang^{1,2}, Zichao Zeng¹, Shenyi Hu¹, Jiaxin Wan¹, Yan Huang³, Fengping Wang⁴, Kurt Konhauser^{5*}, Yinzhaoh Wang^{1,2*}

¹State Key Laboratory of Microbial Metabolism, School of Life Sciences and Biotechnology, Shanghai Jiao Tong University, Shanghai, China.

²Yazhou Bay Institute of Deepsea Science and Technology, Shanghai Jiao Tong University, Shanghai, China.

³Key Laboratory of Development and Application of Rural Renewable Energy, Biogas Institute of Ministry of Agriculture and Rural Affairs, Chengdu, China.

⁴School of Oceanography, Shanghai Jiao Tong University, Shanghai, China.

⁵Department of Earth and Atmospheric Sciences, University of Alberta, Edmonton, Alberta, Canada.

Supplementary information

Environmental distribution and methane-metabolisms of Class II methanogens

SC-*Methanomicrobia* has 11 family-level members. Based on previous research, they are considered as hydrogenotrophic methanogens that utilizing hydrogen to reduce carbon dioxide into methane⁸³⁻⁸⁶. They are distributed in various environments including freshwater or marine sediments⁸⁶⁻⁸⁹, wastewater treatment plant⁹⁰, oil well⁹¹, gas fields⁹², swamp⁹³, sludge⁹⁴ and are even animal-associated⁹⁵.

SC-*Methanosarcinia* is classified into four main clades (in total eight families) (Figure 1). (i)The clade *Methanosarcinia_A* comprises one family named *Methermicoccaceae*. This clade is considered to use methoxylated coal compounds (R-O-CH₃) to produce methane and it was discovered in extreme environments such as Shengli oilfield in China⁹⁶, as well as hydrothermal vent sediments from Guaymas Basin⁹⁷. (ii)*Methanotrichales* clade comprises one family but 11 genus-level lineages. They are considered obligate acetotrophic methanogens that thrive in freshwater environments but can grow in a diverse range of habitats^{95,98-100}. (iii)*Methanosarcinaceae* is a metabolically versatile group¹⁰¹, containing four types of methanogenic pathways including carbon dioxide-reducing, methyl-reducing, methyl-dismutating and acetate-cleaving^{101,102}, and one type of methanotroph. Methanogens of *Methanosarcinaceae* normally dominates in marine water and sediment¹⁰³, and also live in multiple niches such as freshwater¹⁰³, terrestrial soil systems¹⁰⁴, wetland¹⁰⁵, host-related¹⁰⁶, and bioreactors¹⁰⁷. Methanotroph of *Methanosarcinaceae*, ANME-3, lives in methane-rich mud volcanoes¹⁰⁸. (iv)Intriguingly, there is also an entire major multi-order-level clade in SC-*Methanosarcinia* that function as anaerobic methane oxidizers¹⁰⁹. These archaea use reversed methanogenic pathway to oxidize methane coupled with sulfate^{110,111}, nitrate/nitrite, and iron and manganese oxides^{112,113}.

Comparative genomics of SC-*Methanomicrobia* and SC-*Methanosarcinia*

SC-*Methanomicrobia* and SC-*Methanosarcinia* are phylogenetically closely related clades and share comparable average genomic sizes, measuring 2.09 and 2.16 Mb, respectively (Supplementary Figure 13). Nevertheless, they exhibit significant differences in the GC content ($p < 0.0001$) and the frequency of amino acid (AA) utilization (Supplementary Figure 14). The GC content is considered to be related to various ecological factors, such as host association¹¹⁴, oxidative adaption^{115,116}, nitrogen fixing¹¹⁷, and thermal adaptability¹¹⁸. In this context, SC-*Methanomicrobia*

displays a higher average GC content than SC-*Methanosarcinia*, suggesting that the divergence of these major clades has undergone specific evolutionary selective pressures. In addition, substantial alterations in AA utilization frequencies, including glutamic acid, threonine, lysine, proline, asparagine, cystine and alanine, imply that these two superclasses may have adapted to distinct ecological niches, leading to changes in their preferences for these amino acids.

For comparative genomics, a total of 6,851 orthogroups were derived from 70 genomes through OrthoFinder¹¹⁹ and annotated by eggNOG mapper¹²⁰ (Supplementary Figure 13). Among these orthogroups, 924 were identified as the core genome of SC-*Methanosarcinia*, while 1,041 orthogroups constituted the core genome of SC-*Methanomicrobia*. Whereas a total of 4,492 and 3,892 orthogroups compromised the accessory genomes of SC-*Methanosarcinia* and SC-*Methanomicrobia*, respectively. Additionally, these two superclasses shared 789 orthogroups categorized as “common core orthogroups”. For each superclass-specific gene, using a relaxed definition that orthogroups are present in at least 70% of genomes from one superclass but fewer than 30% of genomes from the other superclass, we found 86 and 97 orthogroups form superclass-specific genomes of SC-*Methanosarcinia* and SC-*Methanomicrobia*, respectively (Supplementary Figure 13).

In general, the common core genes found in SC-*Methanosarcinia* and SC-*Methanomicrobia* predominantly participate in fundamental processes such as cell division, vitamin synthesis, transcription, translation, and carbon fixation (Supplementary Table 4). Notably, the core genome of SC-*Methanosarcinia* is smaller than that of SC-*Methanomicrobia* but exhibits a larger set of accessory genes. This discrepancy suggests that the SC-*Methanosarcinia* lineage possesses a more extensive and diversified metabolism potentials compared to SC-*Methanomicrobia*. Indeed, most accessory genes in both superclasses are classified as metabolic substrate transporters, indicating their distinct habitats. Within SC-*Methanosarcinia*, there are distinctive accessory genes related to cytochrome, including Ccm proteins for cytochrome *c* assembly, polyvinyl alcohol dehydrogenase (cytochrome), cytochrome *c*, and cytochrome *c* peroxidase (Supplementary Table 5). In contrast, SC-*Methanomicrobia* contains specific accessory genes for lactate permease, alanine dehydrogenase, and subunits of energy-converting hydrogenase A (Eha) (Supplementary Table 6).

Regarding the genes specific to each superclass, SC-*Methanosarcinia* exhibits significant enrichment in glycerophospholipid, cysteine, and methionine metabolism ($p < 0.05$) (Supplementary Table 7). We observed that members of this superclass also

encode the exosome complex component CSL4/RRP41, which functions as a digester of exogenous RNA, and membrane-bound serine protease that cleaves extracellular substrates. These components play roles in maintaining small molecule homeostasis, self-protection, and the supplementation of growth materials. Moreover, SC-*Methanosarcinia* uniquely possesses membrane-bound proteins for methanogenesis, including the cytochrome subunit (HdrE) of heterodisulfide reductase (HdrDE) and subunits of Fd or F₄₂₀:methanophenazine oxidoreductase (Fpo). In SC-*Methanomicrobia*, genes specific to this superclass significantly enrich in bacterial motility proteins and seleno-compound metabolism ($p < 0.05$) (Supplementary Table 8). Additionally, some archaeal flagellin and chemotaxis proteins are conserved, indicating a strong motility trait within this superclass. Similarly, proteins related to hydrogenase synthesis (Hyp complex) and certain hydrogenases like F₄₂₀-reducing hydrogenase complex (Frh) and methyl-viologen-reducing hydrogenase (Mvh) are conserved.

Contrast methane metabolic pathways between SC-*Methanomicrobia* and SC-*Methanosarcinia*

For SC-*Methanomicrobia*, nearly all genomes contain genes coding for enzymes responsible for catalyzing methane production from hydrogen and carbon dioxide. These genes code for the Wood-Ljungdahl methyl branch (WL-MB) pathway, tetrahydromethanopterin S-methyl-transferase (Mtr) complex, and Mcr, to compose carbon dioxide-reducing hydrogenotrophic methanogenesis pathway (Supplementary Figure 5). However, two exceptions are observed in the genera *JAFGOM01* and *Methanocella_A* which possesses the *mtaB* gene potentially coding for methyltransferase, although experimental verification is lacking.

In SC-*Methanosarcinia*, six families (*Methermicoccaceae*, *Methanotrichaceae*, *Methanocomedenaceae*, *Methanogasteraceae*, *Methanoperedenaceae*, *Methanosarciniaceae*) contain genes associated with the carbon dioxide-reducing hydrogenotrophic methanogenesis pathway (Supplementary Figure 5). Two families, *Methanosarcinaceae* and *Methermicoccaceae*, demonstrate the ability to dismutate methyl compounds for methane production. Almost all species within *Methanosarcinaceae* contain methyltransferases for methylamine (MtmB, MtbB, MttB) and methanol (MtaB), implying a coherent occurrence of methanogenesis from methylamine and methanol within this family. *Methermicoccaceae* species also have *mtmB*, *mtbB*, and *mttB* genes, indicating the potential for methane production from methylamine compounds.

Interestingly, most species from both superclasses contain either two potential pathways of the acetate-cleaving methanogenesis related genes. These pathways include one with genes coding for acetyl-CoA synthase (Acs) and carbon dioxide dehydrogenase complex (Cdh), as well as another with genes for acetate kinase (AckA), phosphoacetyl-transferase (Pta) and Cdh (Supplementary Figure 5). Within SC-*Methanomicrobia*, eight families (*Ca. Methanoflorenceae*, *Methanocellaceae*, *Methanofollaceae*, *JACTUA01*, *Methanosphaerulaceae*, *Methanoculleaceae*, *Methanospirillaceae*, and *Methanoregulaceae*) possess genes necessary for the first type acetate-cleaving methanogenesis pathway. They contain the *acs* gene obtained from the *Bacteria* domain and *cdhABCDE* obtained from *Thermoproteota* or *Hadarchaeota* (Supplementary Figure 15). In SC-*Methanosarcinia*, seven families (*Methermicoccaceae*, *Methanotrichaceae*, *EX4572-44*, *Methanocomedenaceae*, *Methanogasteraceae*, *Methanoperedenaceae*, and *Methanosarciniaceae*) encode the Acs acquired from the *Bacteria* domain and the Cdh complex acquired from *Archaeoglobi* (*cdhABC*) and *Methanoliparia* (*cdhDE*) (Supplementary Figure 15). However, as for now, only *Methanotrichaceae* has been confirmed capable of utilizing acetate as a methanogenic substrate in the first type of acetate-metabolizing pathway⁹⁸⁻¹⁰⁰, whereas other members with these genes, such as *Methanolobus*¹²¹ and *Methanococcoides*¹²², have not been experimentally verified. In addition, two genera, *Methanosarcina* and *MTP4* from *Methanosarcinaceae*, are found to encode genes for the second type of acetate-cleaving methanogenesis with enzymes AckA, and this has been experimentally confirmed in *Methanosarcina*.

Contrast energy system between SC-*Methanomicrobia* and SC-*Methanosarcinia*

Methanogens derive energy from methanogenesis through chemiosmotic energy conservation, coupling the exergonic reactions in the pathway and cofactor system with the establishment of an ionic motive force for ATP production¹²³. In methanogenesis, the energy system is composed of two parts:

(1) *energy conversion during carbon substrate conversion*. During the process of gradually catalyzing carbon substrate into methane, MTR complex catalyzes the transfer of methyl-groups from H₄MPT to CoM-SH, and couples this reaction with build-up of Na⁺ motive force for ATP synthesis. MTR is shared by both superclasses (Supplementary Figure 5).

(2) *energy conversion during cofactors redox reactions*. The Class II methanogens primarily utilize four cofactors in methanogenesis, *i.e.* ferredoxin (Fd_{red/ox}), deazaflavin hydride carrier coenzyme (F₄₂₀), coenzyme B, and coenzyme M

(CoB/CoM). These two superclasses use distinct sets of cofactor enzymes. In SC-*Methanomicrobia*, hydrogenases such as Mvh and Ech are widely utilized for redox reactions of $\text{Fd}_{\text{red/ox}}$, while Frh is for F_{420} . The cytosolic heterodisulfide reductase HdrABC, coupled with Mvh, regenerates CoB-SH and CoM-SH¹²⁴. Eha is involved in replenishing Fd_{red} ¹²⁵, a process likely to have evolved independently in the class *Methanomicrobia*. In SC-*Methanosarcinia*, hydrogenases are either universally absent or incomplete. Instead, the $\text{Fd}_{\text{red/ox}}$:methanophenazine oxidoreductase complex (Rnf) and $\text{Fd}_{\text{red/ox}}$ or F_{420} :methanophenazine oxidoreductase complex (Fd_Fpo , F_{420_Fpo}) are involved in redox reactions between cofactors ($\text{Fd}_{\text{red/ox}}$ or F_{420}) and fat-soluble electron carriers such as methanophenazine, MP)^{126,127}. HdrABC and the membrane-bound heterodisulfide reductase HdrDE may participate in redox reactions of CoB and CoM. Among the above enzymes, the hydrogenases Eha and Ech in SC-*Methanomicrobia* are involved in energy conversion; the membrane-bound enzymes Rnf, Fd_Fpo , F_{420_Fpo} , HdrDE in SC-*Methanosarcinia* are involved in energy conversion. Notably, these membrane-bound enzymes in SC-*Methanosarcinia* are working in form of ETC. ETC is defined as a set of membrane bound protein complexes arranged in a specific order. It receives electrons from reduced cofactors generated in other metabolic pathways and transfers them from carriers with high redox potential to those with lower potential, using the change in reduction potential to pump protons or sodium ions across the membrane¹²⁸.

The energetic efficiency when combining distinct energy systems with three methanogenic pathways.

The comparison of methanogenesis pathways above reveals that both SC-*Methanosarcinia* and SC-*Methanomicrobia* encompass three types of methanogenic pathways. The differentiation in metabolic types between these two superclasses likely stems from variances of energy systems during cofactor redox reactions. To evaluate the energetic efficiency of hydrogenase-based energy system and ETC-based energy system, we calculate the net standard Gibbs free energy change (ΔG^0) for key steps in organic substrate utilization (methyl compounds or acetate) between SC-*Methanosarcinia* and SC-*Methanomicrobia* (Supplementary Figure 6).

In both methyl-dismutating and acetate-cleaving methanogenesis, organic electron donors follow the oxidizing direction of the WL (WL-MB or WL-CB) pathway, releasing electrons to form Fd_{red} or F_{420}H_2 . These electron carriers require specific pathways to deliver electrons to the final acceptor CoM-S-S-CoB. In SC-*Methanosarcinia*, Rnf or Fpo facilitate the delivery of electrons from Fd_{red} and F_{420}H_2 to MP. Subsequently, these fat-soluble electron carriers deliver electrons to HdrDE,

reducing CoM-S-S-CoB. Consequently, members of *SC-Methanosarcinia* can effectively channel electrons from an organic source into energy through methane production. And the total standard Gibbs free energy change with ETC-based energy system shows the whole process are energy-producing.

Conversely, in *SC-Methanomicrobia*, when considering a methyl compound as the energy source (Supplementary Figure 6), the only energy-conserving step involves the reaction catalyzed by Ech in oxidizing Fd_{red} to Fd_{ox} ($\Delta G^{0'} \approx -15.44$ kJ/mol)¹²⁹. In contrast, the energy-consuming step occurs in the reaction catalyzed by the MTR complex during methyl transfer from CoM-SH to H₄MPT, coupled with the consumption of the sodium motive force ($\Delta G^{0'} \approx 30$ kJ/mol)¹³⁰. When acetate is the energy source, the sole energy-conserving reaction involving the transfer of a methyl-group from H₄MPT to CoM-SH via MTR shows only a slight energy gain ($\Delta G^{0'} \approx -30$ kJ/mol). However, activating acetate into acetyl-CoA via Acs is energy-consuming, costing two ATP ($\Delta G^{0'} \approx 30.54$ kJ/mol)¹³¹. It is evident that the conserved energy is insufficient to cover the consumed energy in both scenarios. Therefore, utilizing organic energy sources for methanogenesis appears impractical in *SC-Methanomicrobia*.

Tracing the energy system differentiation to the common ancestor of Class II methanogens

Within all ETCs utilized in methanogenesis by *SC-Methanosarcinia* (Figure 2), HdrDE represents an essential component, acting as the terminal complex. It receives electrons from MPH₂ to reduce the terminal acceptor CoB-S-S-CoM and is involved in generating a proton chemiosmotic gradient across the cell membrane^{132,133}. The HdrDE complex contains an iron-sulfur protein, HdrD, with catalytic activity, and a cytochrome *b* subunit, HdrE, that mediates electron transmission and proton translocation¹³². We found that the gene coding for HdrDE is ubiquitously distributed across nearly all genomes of *SC-Methanosarcinia* (Supplementary Figure 5). However, HdrD sequences from *SC-Methanosarcinia* form two distinct clades on the phylogenetic tree (Supplementary Figure 7). One clade clusters with *Methanonatronarchaeales*, while the other clade clusters with *Syntropharchaeaceae*, implying that *SC-Methanosarcinia* acquired the HdrD-encoding gene via at least two HGT events. Remarkably, only the gene coding for HdrD homologs to *Methanonatronarchaeales* is co-located with the HdrE-encoding gene (Supplementary Figure 7), suggesting their likely functionality in the normal HdrDE complex. In contrast, HdrD from *Syntropharchaeaceae*, lacking HdrE, may have a different function or be nonfunctional.

Regarding HdrE, it belongs to the protein family PF02665, recognized as a *b*-type cytochrome and the gamma subunit of the nitrate reductase responsible for receiving electrons from the quinone pool in various bacteria¹³³. By detecting and annotating PF02665 sequences across representative archaeal genomes from the GTDB database release 207, we identified roughly four major clades of PF02665 sequences (Supplementary Figure 16). In the Class II methanogens, sequences annotated as HdrE belong to classes *Methanosarcinia* and *Methanosarcinia_A*, as well as in the *Methanoculleaceae*, *Methanosphaerulaceae* and *Methanospirillaceae* families within the class *Methanomicrobia*. HdrE is also present in *Methanonatronarchaeales* and *JACAEJ01* (formerly called *Ca. Methylarchaeales*), anaerobic alkane-oxidizing archaea from families *Syntropharchaeaceae* and *JdFR-42* in *Archaeoglobi*, and isoprenoids producer belonging to the order *UBA10834* in *Thermoplasmata* (formerly called *Ca. Gimiplasmatales*¹³⁴). The phylogenetic tree of the PF02665 family (Supplementary Figure 16) shows that almost all HdrE sequences cluster together, with the exception being the HdrE sequences from *Ca. Methylarchaeales*. They cluster with HmeC sequences from *Thermoproteota*, indicating nonhomology to other HdrE sequences (e-value > 1e-5). For the HdrE-like sequences of unknown function closely clustered with the known HdrE sequences, they also exhibit the domain for HdrD (PF13183: Fer4_8; PF02754: CCG) adjacent to the domain for HdrE (PF02665: Nitrate_red_gam). This suggests that HdrE-like sequences may also have an ETC-related function, even though these microbes lack methane-related metabolisms.

To further investigate the origins of HdrE, we conducted a phylogenetic analysis of HdrE and HdrE-like sequences across the *Archaea* and *Bacteria* domains (Supplementary Figure 8). Most sequences of HdrE and HdrE-like exhibit separative evolutionary histories, forming distinct clusters. However, certain HdrE-like sequences from *Hermodarchaeia* occasionally cluster with HdrE (Supplementary Figure 8). Additionally, domain-crossing HGTs can be observed in both HdrE and HdrE-like clusters. Some bacterial HdrE sequences frequently cluster with archaeal HdrE sequences from *Syntropharchaeaceae*, *Archaeoglobi* and *Thermoplasmata*, suggesting a potential bacterial origin of HdrE-encoding gene. Examining the detailed evolutionary history of HdrE within SC-*Methanosarcinia* (Figure 2), it is estimated that the earliest node at which HdrE in SC-*Methanosarcinia* originated from a HGT event. Specifically, the ancestor of *Methanosarcinia_A* received HdrE transferred from *Methanonatronarchaeales* or another donor that has not yet been identified or is already extinct. Subsequently, this cytochrome spread throughout SC-*Methanosarcinia* primarily through speciation events. Interestingly, *Methanoculleus_A* from SC-*Methanomicrobia* also acquired the HdrE-encoding gene

from *Methanotrichaceae* via an HGT event, thus expanding their metabolic potentials (Figure 2).

The HdrDE complex was first discovered in *Methanosarcina barkeri*¹³⁵, where it played a role in assisting the MCR complex in reducing methyl-coenzyme M to produce CoB-S-S-CoM. Subsequently, genes coding for HdrDE have been found in various methanogens, including those from *Methanosarcinales*¹³⁶, *Methanotrichales*¹³⁷, *Methermicoccus*⁹⁶, and *Ca. Methylarchaeales*¹³⁸ in *Thermoproteota*. Additionally, HdrDE homologues have been found in methanotrophs from *Methansarcinales*^{29,139,140}, alkanotrophs such as *Ca. Polytropus marinfundus* in *Archaeoglobi*¹⁴¹, sulfate reducers from *Archaeoglobus* involved in catalyzing disulfide/thiol conversions of DsrC (a heterodisulfide protein) during sulfate reduction¹⁴²⁻¹⁴⁴, and assisting a specific fumarate reductase using CoM-SH and CoB-SH in *Hermodarchaeota* from Asgard archaea¹⁴⁵. Despite being identified in various microorganisms, the HdrDE complex has only been purified from methanogens¹³⁵, and experimentally verified as functioning in the process of methanogenesis by coupling the heterodisulfide reducing reaction with energy conservation^{146,147}. Owing to HdrDE, hydrogenotrophic SC-*Methanosarcina* species, such as *Methanosarcina barkeri* and *Methanosarcina mazei*, achieve higher energy efficiency by converting the released free energy into a proton motive force during the heterodisulfide reducing reaction. This efficiency, however, requires a higher hydrogen threshold concentration (>100 Pa) compared to SC-*Methanomicrobia* species (<10 Pa)^{102,148}. Considering that diverse metabolic types of methanogenesis that utilize organic energy are characterized for SC-*Methanosarcinia*, in contrast to their sister lineage SC-*Methanomicrobia* and other methanogens (like Class I methanogens) which can only use hydrogen, we propose that the ancestor of Class II methanogens likely conducted hydrogenotrophic methanogenesis. The horizontal transfer of essential ETC genes (*hdrDE*) to the ancestor of SC-*Methanosarcinia* marks the onset of energy system differentiation between two superclasses, allowing SC-*Methanosarcinia* to develop its own ETC.

History of losing ability of hydrogenotrophic living

In SC-*Methanosarcinia*, although the complete gene cluster coding for Hyp is detected in several groups such as *JdFR-19* from *Methanosarcinia_A*, ANME group, and *Methanosarcinaceae*, it is mostly acquired through horizontal gene transfer (Supplementary Figure 3). The phylogeny of Hyp shows that *JdFR-19* obtained Hyp complex genes from *Thermoproteota*. For *Methanosarcinales* (ANME group and *Methanosarcinaceae*), Hyp subunits originated from diverse sources, including the

Class I methanogen (HypA and HypB), SC-*Methanomicrobia* (HypC, HypF), even the Class III methanogen (HypD and HypE). The varied origins of the Hyp complex suggest that SC-*Methanosarcinia* might have lost the *hpyABCDEF* at the period of common ancestor, or at the early stages of sublineages (like ancestor of *Methanosarcinia_A*, ancestor of *Methanotrichales*).

The diversification of ETCs is consistent with metabolic diversification in SC-*Methanosarcinia*

The shift of methanogenesis in SC-*Methanosarcinia* is closely related to ETCs' reforming (Figure 1). Therefore, through phylogenetic analysis of all ETC-concerned enzymes, we conclude the history of methanogenesis diversification along with the phylogenetic diversification of SC-*Methanosarcinia*. The last common ancestor of SC-*Methanosarcinia* has constructed ETC "Fd_Fpo-HdrDE" by acquiring genes of Fpo from archaea and bacteria via HGTs (Supplementary Figure 9). *Methanosarcinia_A* inherited this and utilizes it today to conserve energy by oxidizing Fd_{red} which is formed in the oxidizing direction of the WL-MB pathway and transmitting the electrons to reduce CoM-S-S-CoB in methoxyl-dismutating methanogenesis. Simultaneously, it supplements this process with the electron bifurcation mechanism conducted by HdrABC and FdhB, which transfers electrons from F₄₂₀H₂ to CoM-S-S-CoB (Figure 2). *Methanotrichales* also inherited the "Fd_Fpo-HdrDE" ETC, connecting it to the WL-CB pathway and MCR. This lineage conserves energy by oxidizing Fd_{red} produced by the WL-CB pathway and transmitting the electrons to reduce CoM-S-S-CoB in the acetate-cleaving methanogenesis. The ancestor of *Methanosarcinales* acquired genes coding for Rnf (Supplementary Figure 10) from bacteria and replaced Fd_Fpo with F₄₂₀_Fpo by acquiring the gene coding for FpoF subunit (Supplementary Figure 9). Within *Methanosarcinales*, the evolution of ANME group was estimated to be triggered by the acquisition of genes for cytochrome *b* and cytochrome *c*¹²⁶. This lineage reversed the methanogenic pathway to oxidize methane into carbon dioxide, generating Fd_{red}, F₄₂₀H₂, CoB-SH, and CoM-SH during this process. To access electrons from these reduced carriers to their final electron acceptors, such as sulfate and nitrate, the ANME group reconfigured ETCs into extracellular electron transfer (EETs)¹²⁶ "F₄₂₀_Fpo-cytb-cytc", "Rnf-cytb-cytc", and "HdrDE-cytb-cytc" to transfer electrons from F₄₂₀H₂, Fd_{red}, CoB-SH, and CoM-SH to extracellular sulfate or nitrate (Supplementary Figure 17, Figure 2). In their sister group, *Methanosarcinaceae* effectively inherited Rnf and F₄₂₀_Fpo to construct new ETCs, such as "Rnf-HdrDE" and "F₄₂₀_Fpo-HdrDE", or to conserve energy by oxidizing Fd_{red} and F₄₂₀H₂ for reducing CoM-S-S-CoB, respectively. Moreover, within *Methanosarcinaceae*, three

genera (*Methanimicrococcus*, *Methanosarcina*, and *MTP4*) reacquired the Hyp complex, thereby recovering their ability to synthesize [NiFe] hydrogenase. Based on this, these three genera innovated the new ETC “Vht-HdrDE”, allowing hydric electrons to be reaccepted by final electron acceptor CoM-S-S-CoB. *Methanimicrococcus* and *Methanosarcina* both use “Vht-HdrDE” in methyl-reducing methanogenesis, and some species of *Methanosarcina*, such as *Methanosarcina mazei*¹⁵¹ and *Methanosarcina barkeri*¹⁵² from fresh water, were reported to utilize ETC “Vht-HdrDE” in carbon dioxide-reducing methanogenesis or combine Ech with “Vht-HdrDE” in methyl-dismutating methanogenesis (Supplementary Figure 18).

Reference

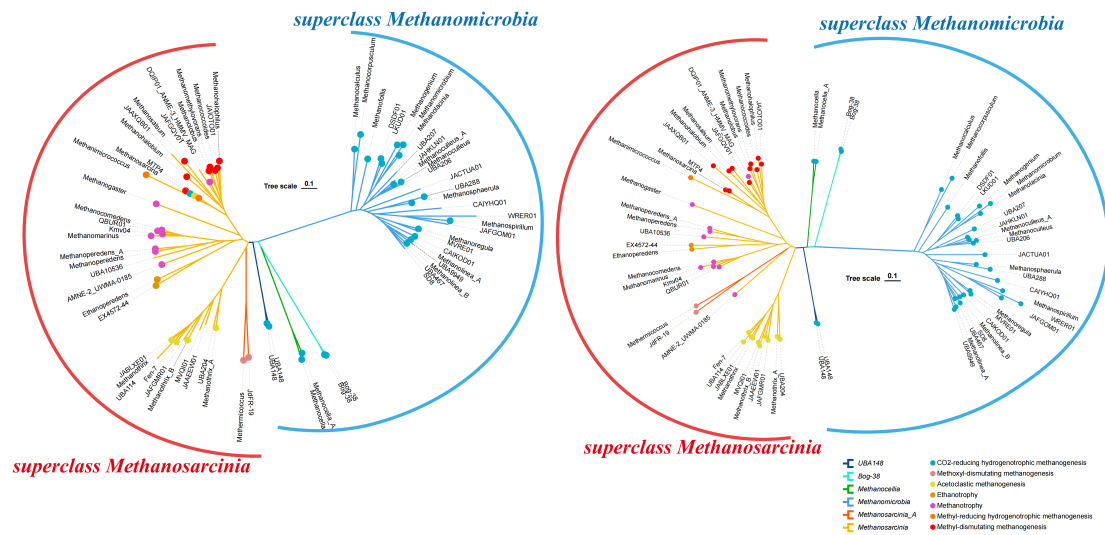
- 83 Liu, Y., Whitman, W. B. Metabolic, phylogenetic, and ecological diversity of the methanogenic archaea. *Ann. N. Y. Acad. Sci.* **1125**, 171-189 (2008).
- 84 Mondav, R., Woodcroft, B. J., Kim, E. H., et al. Discovery of a novel methanogen prevalent in thawing permafrost. *Nat. Commun.* **5**, 3212 (2014).
- 85 Parks, D. H., Rinke, C., Chuvochina, M. et al. Recovery of nearly 8,000 metagenome-assembled genomes substantially expands the tree of life. *Nat. Microbiol.* **2**, 1533-1542 (2017).
- 86 Sakai, S., Conrad, R., Liesack, W. et al. *Methanocella arvoryzae* sp. nov., a hydrogenotrophic methanogen isolated from rice field soil. *Int. J. Syst. Evol. Microbiol.* **60**, 2918-2923 (2010).
- 87 Lai, M. C., Chen, S. C., Shu, C. M. et al. *Methanocalculus taiwanensis* sp. nov., isolated from an estuarine environment. *Int. J. Syst. Evol. Microbiol.* **52**, 1799-1806 (2002).
- 88 Lai, M. C., Lin, C. C., Yu, P. H. et al. *Methanocalculus chunghsingensis* sp. nov., isolated from an estuary and a marine fishpond in Taiwan. *Int. J. Syst. Evol. Microbiol.* **54**, 183-189 (2004).
- 89 Sakai, S., Takaki, Y., Shimamura, S. et al. Genome sequence of a mesophilic hydrogenotrophic methanogen *Methanocella paludicola*, the first cultivated representative of the order Methanocellales. *PLoS ONE* **6**, e22898 (2011).
- 90 Zellner, G., Stackebrandt, E., Messner, P. et al. Methanocorpusculaceae fam. nov., represented by *Methanocorpusculum parvum*, *Methanocorpusculum sinense* spec. nov. and *Methanocorpusculum bavaricum* spec. nov. *Arch. Microbiol.* **151**, 381-390 (1989).
- 91 Dengler, L., Meier, J., Grünberger, F. et al. *Methanofollis propanolicus* sp. nov., a novel archaeal isolate from a Costa Rican oil well that uses propanol for methane production. *Arch. Microbiol.* **204**, 554 (2022).
- 92 Mochimaru, H., Tamaki, H., Katayama, T. et al. *Methanomicrobium antiquum* sp. nov., a hydrogenotrophic methanogen isolated from deep sedimentary aquifers in a natural gas field. *Int. J. Syst. Evol. Microbiol.* **66**, 4873-4877 (2016).
- 93 Göker, M., Lu, M., Fiebig, A., et al. Genome sequence of the mud-dwelling archaeon *Methanoplanus limicola* type strain (DSM 2279(T)), reclassification of *Methanoplanus petrolearius* as *Methanolacinia petrolearia* and emended descriptions of the genera *Methanoplanus* and *Methanolacinia*. *Stand. Genomic Sci.* **9**, 1076-1088 (2014).
- 94 Botello Suárez, W. A., da Silva Vantini, J., Duda, R. M., et al. Predominance of syntrophic bacteria, *Methanosaeta* and *Methanoculleus* in a two-stage up-flow anaerobic sludge blanket reactor treating coffee processing wastewater at high organic loading rate. *Bioresour. Technol.* **268**, 158-168 (2018).
- 95 Volmer, J. G., Soo, R. M., Evans, P. N. et al. Isolation and characterisation of novel *Methanocorpusculum* species indicates the genus is ancestrally host-associated. *BMC Biol.* **21**, 59 (2023).
- 96 Cheng, L., Qiu, T. L., Yin, X. B. et al. *Methermicoccus shengliensis* gen. nov., sp. nov., a thermophilic, methylotrophic methanogen isolated from oil-production water, and proposal of *Methermicoccaceae* fam. nov. *Int. J. Syst. Evol. Microbiol.* **57**, 2964-2969 (2007).

- 97 Lever, M. A., Teske, A. P. Diversity of methane-cycling archaea in hydrothermal sediment investigated by general and group-specific PCR primers. *Appl. Environ. Microbiol.* **81**, 1426-1441 (2015).
- 98 Berger, S., Welte, C., Deppenmeier, U. Acetate activation in *Methanosaeta thermophila*: characterization of the key enzymes pyrophosphatase and acetyl-CoA synthetase. *Archaea* **2012**, 315153 (2012).
- 99 Liu, C., Sun, D., Zhao, Z. et al. Methanotrix enhances biogas upgrading in microbial electrolysis cell via direct electron transfer. *Bioresour. Technol.* **291**, 121877 (2019).
- 100 Jetten, M. S. M., Stams, A. J. M., Zehnder, A. J. B. Methanogenesis from acetate: a comparison of the acetate metabolism in *Methanotrix soehngenii* and *Methanosarcina* spp. *FEMS Microbiol. Lett.* **88**, 181-197 (1992).
- 101 Garcia, P. S., Gribaldo, S., Borrel, G. Diversity and Evolution of Methane-Related Pathways in Archaea. *Annu. Rev. Microbiol.* **76**, 727-755 (2022).
- 102 Thauer, R. K., Kaster, A. K., Seedorf, H. et al. Methanogenic archaea: ecologically relevant differences in energy conservation. *Nat. Rev. Microbiol.* **6**, 579-591 (2008).
- 103 Yin, X., Wu, W., Maeke, M., et al. CO₂ conversion to methane and biomass in obligate methylotrophic methanogens in marine sediments. *ISME J.* **13**, 2107-2119 (2019).
- 104 Angel, R., Matthies, D., Conrad, R. Activation of methanogenesis in arid biological soil crusts despite the presence of oxygen. *PLoS ONE* **6**, e20453 (2011).
- 105 Angle, J. C., Morin, T. H., Solden, L. M. et al. Methanogenesis in oxygenated soils is a substantial fraction of wetland methane emissions. *Nat. Commun.* **8**, 1567 (2017).
- 106 Thomas, C. M., Taib, N., Gribaldo, S. et al. Comparative genomic analysis of *Methanimicrococcus blatticola* provides insights into host adaptation in archaea and the evolution of methanogenesis. *ISME Commun.* **1**, 47 (2021).
- 107 Fu, S., Lian, S., Angelidaki, I. et al. Micro-aeration: an attractive strategy to facilitate anaerobic digestion. *Trends Biotechnol.* **41**, 714-726 (2023).
- 108 Lösekann, T., Knittel, K., Nadalig, T. et al. Diversity and abundance of aerobic and anaerobic methane oxidizers at the Haakon Mosby Mud Volcano, Barents Sea. *Appl. Environ. Microbiol.* **73**, 3348-3362 (2007).
- 109 Hahn, C. J., Laso-Pérez, R., Vulcano, F. et al. "Candidatus *Ethanoperedens*," a thermophilic genus of archaea mediating the anaerobic oxidation of ethane. *mBio* **11** (2020).
- 110 McGlynn, S. E. Energy metabolism during anaerobic methane oxidation in ANME archaea. *Microbes Environ.* **32**, 5-13 (2017).
- 111 Orphan, V. J., House, C. H., Hinrichs, K. U. et al. Multiple archaeal groups mediate methane oxidation in anoxic cold seep sediments. *Proc. Natl. Acad. Sci. U.S.A* **99**, 7663-7668 (2002).
- 112 Leu, A. O., McIlroy, S. J., Ye, J. et al. Lateral gene transfer drives metabolic flexibility in the anaerobic methane-oxidizing archaeal family *Methanoperedenaceae*. *mBio* **11** (2020).
- 113 Cai, C., Ni, G., Xia, J. et al. Response of the anaerobic methanotrophic archaeon *Candidatus "Methanoperedens nitroreducens"* to the long-term ferrihydrite amendment. *Front. Microbiol.* **13**, 799859 (2022).
- 114 Moran, N. A. Microbial minimalism: genome reduction in bacterial pathogens. *Cell* **108**, 583-586 (2002).

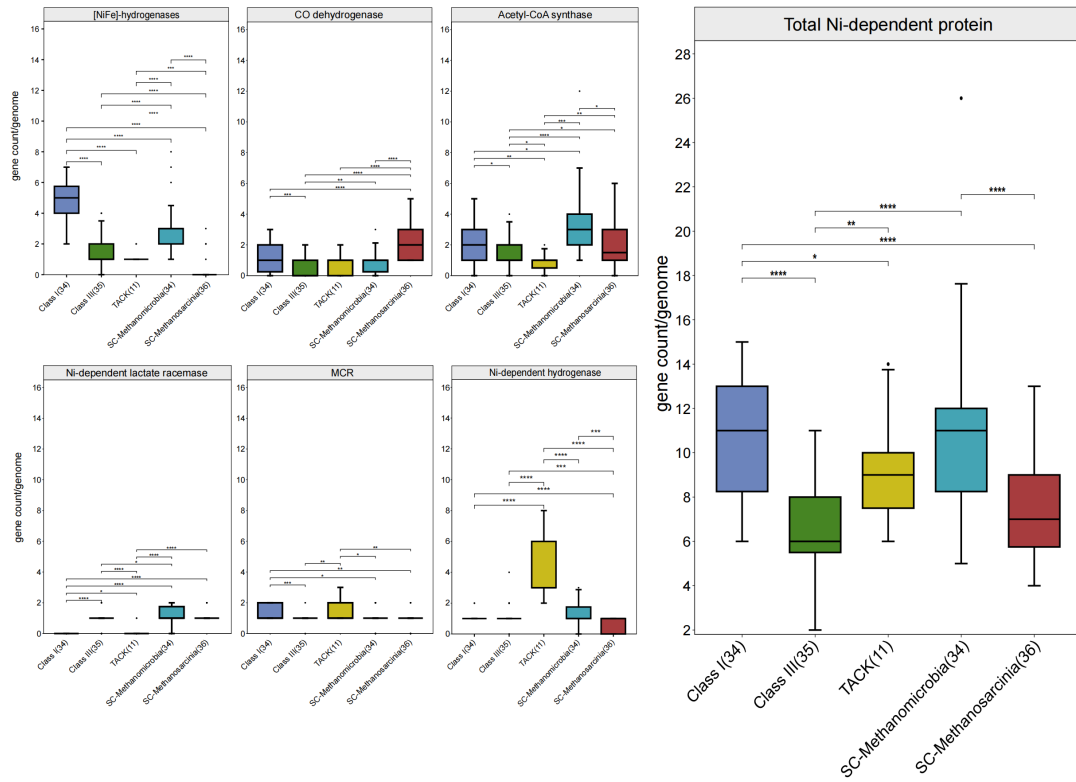
- 115 Naya, H., Romero, H., Zavala, A. et al. Aerobiosis increases the genomic guanine plus
cytosine content (GC%) in prokaryotes. *J. Mol. Evol.* **55**, 260-264 (2002).
- 116 Aslam, S., Lan, X. R., Zhang, B. W. et al. Aerobic prokaryotes do not have higher GC
contents than anaerobic prokaryotes, but obligate aerobic prokaryotes have. *BMC Evol.
Biol.* **19**, 35 (2019).
- 117 McEwan, C. E., Gatherer, D., McEwan, N. R. Nitrogen-fixing aerobic bacteria have higher
genomic GC content than non-fixing species within the same genus. *Hereditas* **128**,
173-178 (1998).
- 118 Musto, H., Naya, H., Zavala, A. et al. Correlations between genomic GC levels and
optimal growth temperatures in prokaryotes. *FEBS Lett.* **573**, 73-77 (2004).
- 119 Emms, D. M., Kelly, S. OrthoFinder: phylogenetic orthology inference for comparative
genomics. *Genome Biol.* **20**, 238 (2019).
- 120 Huerta-Cepas, J., Forslund, K., Coelho, L. P. et al. Fast genome-wide functional
annotation through orthology assignment by eggNOG-Mapper. *Mol. Biol. Evol.* **34**,
2115-2122 (2017).
- 121 Shen, Y., Chen, S. C., Lai, M. C. et al. *Methanolobus halotolerans* sp. nov., isolated from
the saline Lake Tus in Siberia. *Int. J. Syst. Evol. Microbiol.* **70**, 5586-5593 (2020).
- 122 Liang, L., Sun, Y., Dong, Y. et al. *Methanococcoides orientis* sp. nov., a methylotrophic
methanogen isolated from sediment of the East China Sea. *Int. J. Syst. Evol. Microbiol.*
72 (2022).
- 123 Mand, T. D., Metcalf, W. W. Energy conservation and hydrogenase function in
methanogenic archaea, in particular the genus *Methanosarcina*. *Microbiol. Mol. Biol. Rev.*
83 (2019).
- 124 Kaster, A. K., Moll, J., Parey, K. et al. Coupling of ferredoxin and heterodisulfide reduction
via electron bifurcation in hydrogenotrophic methanogenic archaea. *Proc. Natl. Acad.
Sci. U.S.A* **108**, 2981-2986 (2011).
- 125 Lie, T. J., Costa, K. C., Lupa, B. et al. Essential anaplerotic role for the energy-converting
hydrogenase Eha in hydrogenotrophic methanogenesis. *Proc. Natl. Acad. Sci. U.S.A* **109**,
15473-15478 (2012).
- 126 Chadwick, G. L., Skennerton, C. T., Laso-Perez, R. et al. Comparative genomics reveals
electron transfer and syntrophic mechanisms differentiating methanotrophic and
methanogenic archaea. *PLoS Biol.* **20**, e3001508 (2022).
- 127 Welte, C., Deppenmeier, U. . Membrane-bound electron transport in *Methanosaeta*
thermophila. *J. Bacteriol.* **193**, 2868-2870 (2011).
- 128 Nolfi-Donagan, D., Braganza, A., Shiva, S. Mitochondrial electron transport chain:
Oxidative phosphorylation, oxidant production, and methods of measurement. *Redox
Biol.* **37**, 101674 (2020).
- 129 Welte, C., Krätzer, C., Deppenmeier, U. . Involvement of Ech hydrogenase in energy
conservation of *Methanosarcina mazei*. *FEBS J.* **277**, 3396-3403 (2010).
- 130 Welte, C., Deppenmeier, U. Bioenergetics and anaerobic respiratory chains of aceticlastic
methanogens. *Biochim. Biophys. Acta.* **1837**, 1130-1147 (2014).
- 131 Schlegel, K., Müller, V. Evolution of Na⁺ and H⁺ bioenergetics in methanogenic archaea.
Biochem. Soc. Trans. **41**, 421-426 (2013).
- 132 Hedderich, R., Hamann, N., Bennati, M. Heterodisulfide reductase from methanogenic

- archaea: a new catalytic role for an iron-sulfur cluster. *Biol. Chem.* **386**, 961-970 (2005).
- 133 Pantel, I., Lindgren, P-E., Neubauer, H. et al. Identification and characterization of the
Staphylococcus carnosus nitrate reductase operon. *Mol. Gen. Genet.* **259**, 105-114
(1998).
- 134 Hu, W., Pan, J., Wang, B., et al. Metagenomic insights into the metabolism and evolution
of a new Thermoplasmata order (Candidatus Gimiplasmatales). *Environ. Microbiol.* **23**,
3695-3709 (2021).
- 135 Heiden, S., Hedderich, R., Setzke, E., et al. Purification of a cytochrome b containing
H₂:heterodisulfide oxidoreductase complex from membranes of Methanosarcina barkeri.
Eur. J. Biochem. **213**, 529-535 (1993).
- 136 Yan, Z., Ferry, J. G. Electron bifurcation and confurcation in methanogenesis and reverse
methanogenesis. *Front. Microbiol.* **9**, 1322 (2018).
- 137 Welte, C., Deppenmeier, U. Membrane-Bound Electron Transport in Methanosaeta
thermophila. *J. Bacteriol.* **193**, 2868-2870 (2011).
- 138 Ou, Y. F., Dong, H. P., McIlroy, S. J. et al. Expanding the phylogenetic distribution of
cytochrome b-containing methanogenic archaea sheds light on the evolution of
methanogenesis. *ISME J.* (2022).
- 139 Wang, F. P., Zhang, Y., Chen, Y. et al. Methanotrophic archaea possessing diverging
methane-oxidizing and electron-transporting pathways. *ISME J.* **8**, 1069-1078 (2014).
- 140 Leu, A. O., Cai, C., McIlroy, S. J. et al. Anaerobic methane oxidation coupled to
manganese reduction by members of the Methanoperedenaceae. *ISME J.* **14**, 1030-
1041 (2020).
- 141 Boyd, J. A., Jungbluth, S. P., Leu, A. O. et al. Divergent methyl-coenzyme M reductase
genes in a deep-subseafloor Archaeoglobi. *ISME J.* **13**, 1269-1279 (2019).
- 142 Mander, G. J., Duin, E. C., Linder, D. et al. Purification and characterization of a
membrane-bound enzyme complex from the sulfate-reducing archaeon Archaeoglobus
fulgidus related to heterodisulfide reductase from methanogenic archaea. *Eur. J.*
Biochem. **269**, 1895-1904 (2002).
- 143 Mander, G. J., Duin, E. C., Linder, D., et al. Purification and characterization of a
membrane-bound enzyme complex from the sulfate-reducing archaeon Archaeoglobus
fulgidus related to heterodisulfide reductase from methanogenic archaea. *Eur. J.*
Biochem. **269**, 1895-1904 (2002).
- 144 Hocking, W. P., Stokke, R., Roalkvam, I. et al. Identification of key components in the
energy metabolism of the hyperthermophilic sulfate-reducing archaeon Archaeoglobus
fulgidus by transcriptome analyses. *Front. Microbiol.* **5**, 95 (2014).
- 145 Zhang, J. W., Dong, H. P., Hou, L. J. et al. Newly discovered Asgard archaea
Hermodarchaeota potentially degrade alkanes and aromatics via alkyl/benzyl-succinate
synthase and benzoyl-CoA pathway. *ISME J.* **15**, 1826-1843 (2021).
- 146 Kröninger, L., Berger, S., Welte, C. et al. Evidence for the involvement of two
heterodisulfide reductases in the energy-conserving system of Methanomassiliicoccus
luminyensis. *FEBS J.* **283**, 472-483 (2016).
- 147 Wang, M., Tomb, J. F., Ferry, J. G. Electron transport in acetate-grown Methanosarcina
acetivorans. *BMC Microbiol.* **11**, 165 (2011).
- 148 Thauer, R. K., Kaster, A. K., Goenrich, M. et al. Hydrogenases from methanogenic archaea,

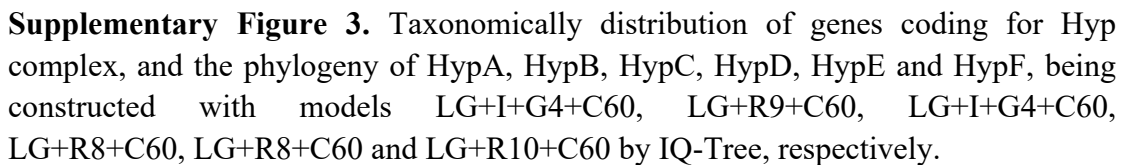
- nickel, a novel cofactor, and H₂ storage. *Annu. Rev. Biochem.* **79**, 507-536 (2010).
- 149 Miki, K., Atomi, H., Watanabe, S. Structural Insight into [NiFe] Hydrogenase Maturation
by Transient Complexes between Hyp Proteins. *Acc. Chem. Res.* **53**, 875-886 (2020).
- 150 Montag, D., Schink, B. Formate and hydrogen as electron shuttles in terminal
fermentations in an oligotrophic freshwater lake sediment. *Appl. Environ. Microbiol.* **84**
(2018).
- 151 Welte, C., Kallnik, V., Grapp, M. et al. Function of Ech hydrogenase in ferredoxin-
dependent, membrane-bound electron transport in *Methanosarcina mazei*. *J. Bacteriol.*
192, 674-678 (2010).
- 152 Meuer, J., Bartoschek, S., Koch, J. et al. Purification and catalytic properties of Ech
hydrogenase from *Methanosarcina barkeri*. *Eur. J. Biochem.* **265**, 325-335 (1999).



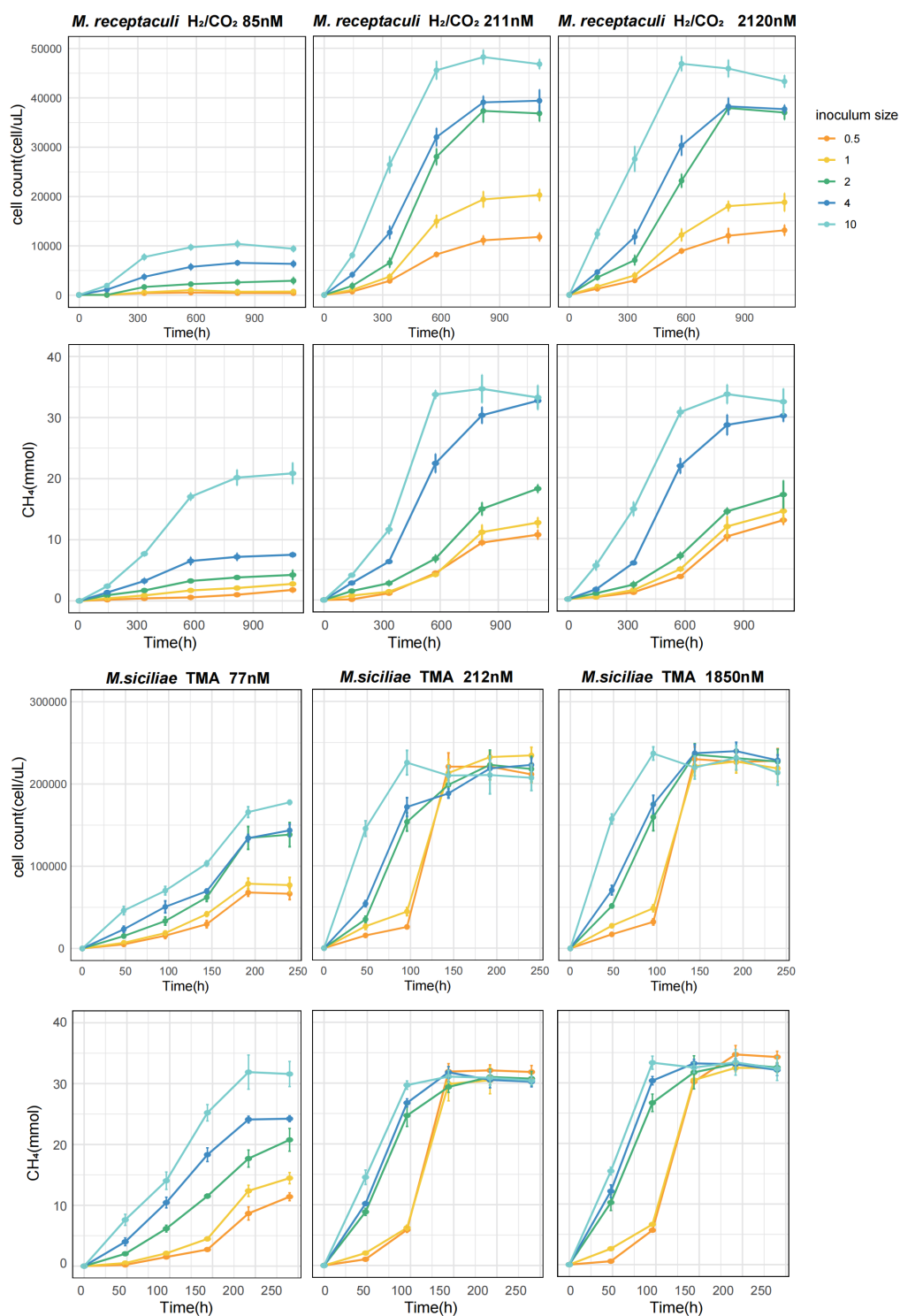
Supplementary Figure 1. Unrooted phylogenetic trees of Class II methanogen. On the basis of the concatenated alignment of a set of 37 (left) and 53 (right) conserved marker genes, the tree is constructed with model LG+R8+C60 and LG+F+R8+C60, respectively, by IQ-Tree.



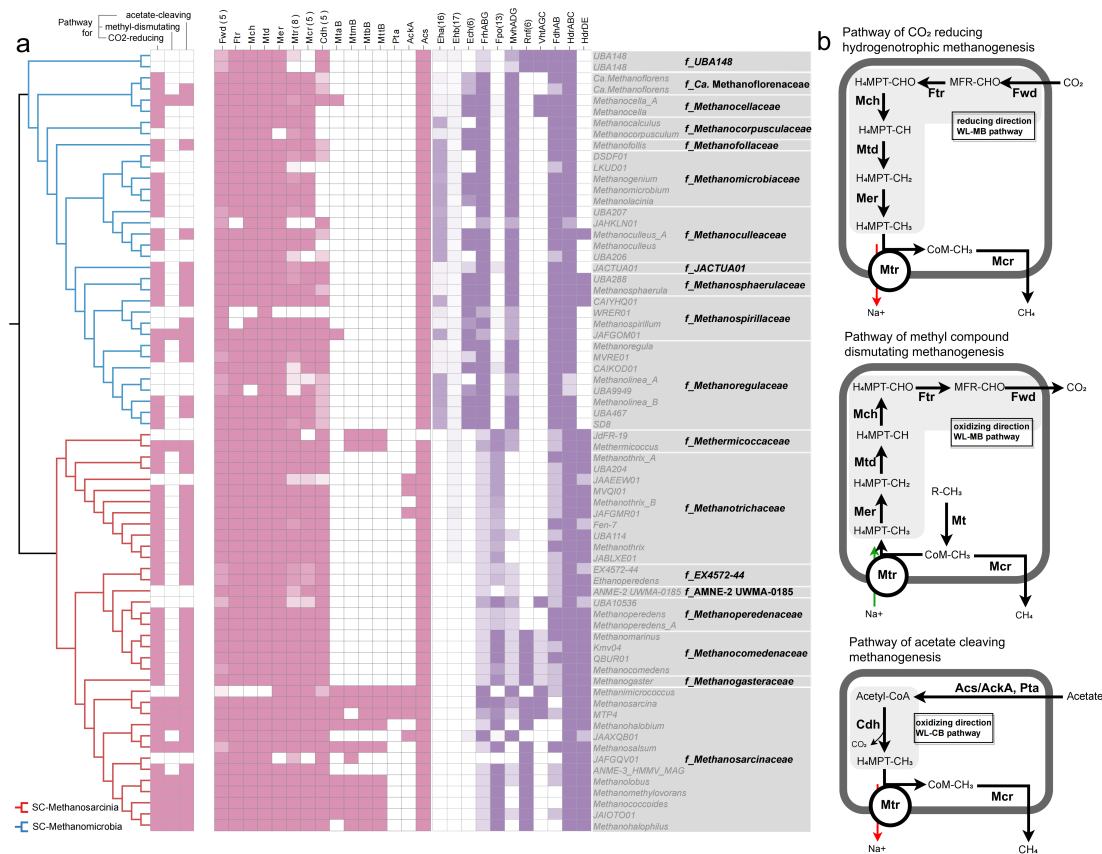
Supplementary Figure 2. Boxplots of gene count of nickel-dependent enzymes in different methanogen groups, including Class I, Class III, TACK, SC-*Methanosarcinia* and SC-*Methanomicrobia*. The nickel-containing proteins from [NiFe]-hydrogenases (EchE, EhaO, FrhA, MvhA, VhoA), CO dehydrogenase (CdhA, CooS), MCR (McrA), Acetyl-CoA synthase (Acs), Ni-dependent lactate racemase (LarA) and Ni-dependent hydrogenase (AraM, MbhL etc.) are calculated respectively, and the total gene count of above proteins are also calculated. Stars represent the significant differences between two superclasses, determined using a Wilcoxon test.



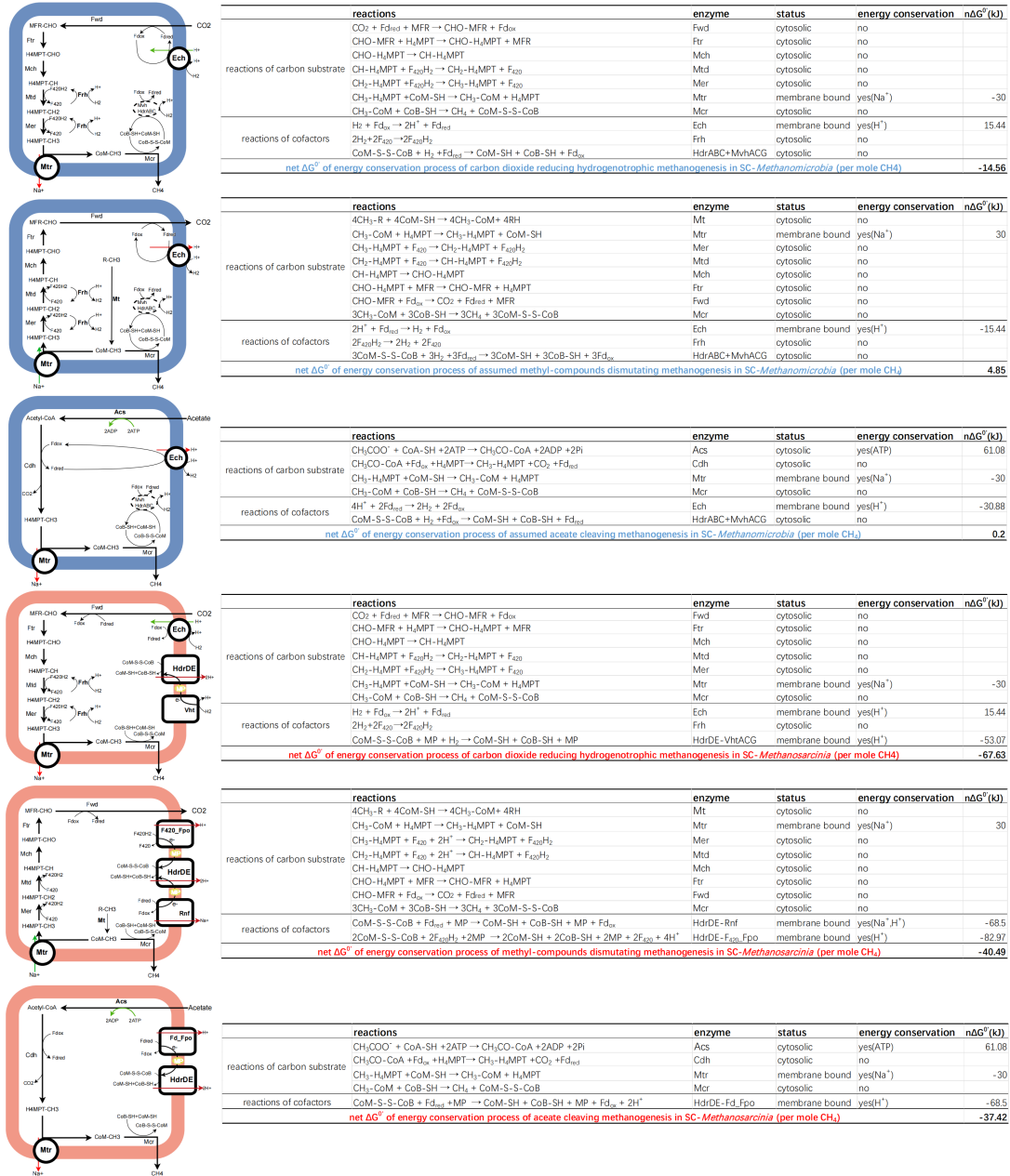
Supplementary Figure 3. Taxonomically distribution of genes coding for Hyp complex, and the phylogeny of HypA, HypB, HypC, HypD, HypE and HypF, being constructed with models LG+I+G4+C60, LG+R9+C60, LG+I+G4+C60, LG+R8+C60, LG+R8+C60 and LG+R10+C60 by IQ-Tree, respectively.



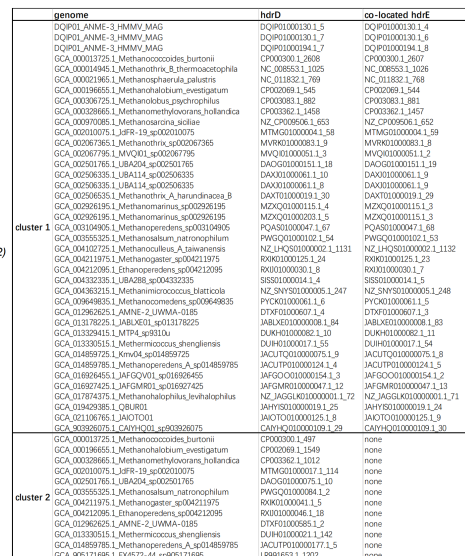
Supplementary Figure 4. Methane production and cell proliferation of *M.siciliae* and *M.receptaculi* growing under different nickel level. Both strains are cultured with 0.5%, 1%, 2%, 4%, 10% inoculum size.



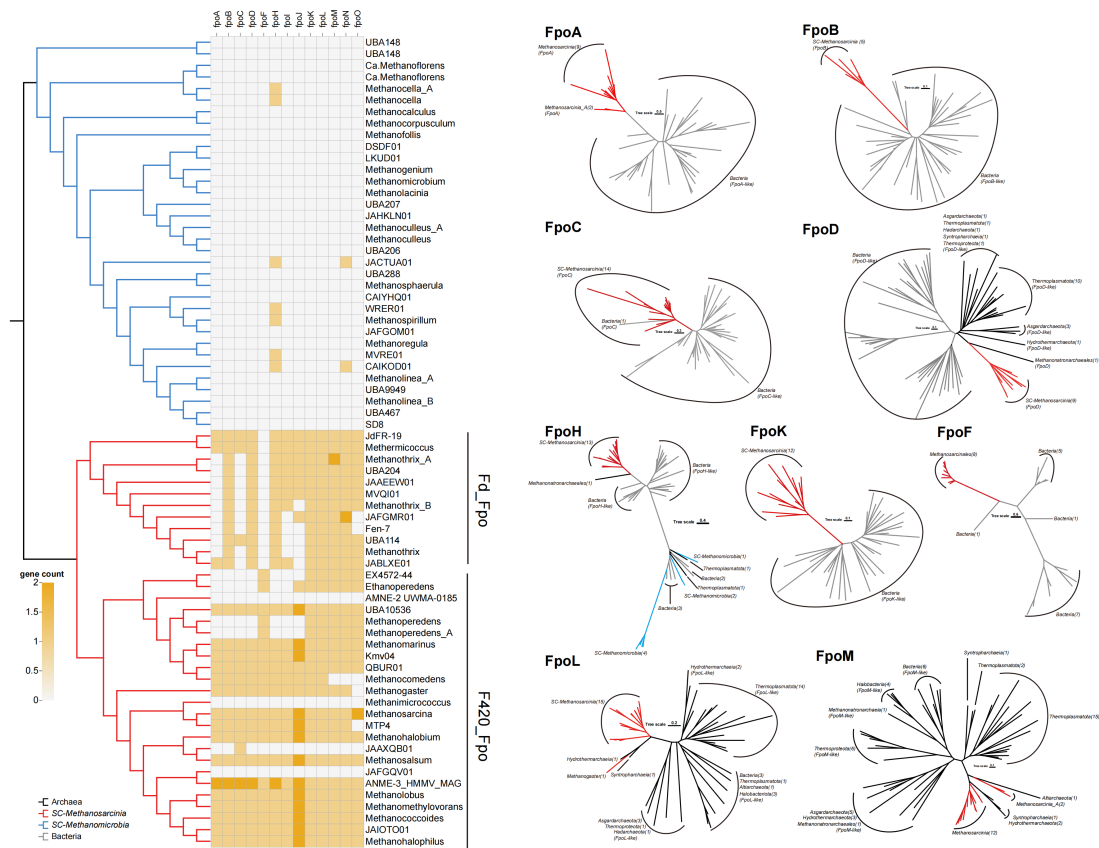
Supplementary Figure 5. Comparative analysis of three types of methanogenesis. (a) Heatmaps of methanogenesis-relate genes, showing the taxonomically distribution of carbon dioxide reducing hydrogenotrophic, methyl-dismutating and acetate-cleaving methanogenesis across the phylogeny of SC-*Methanomicrobia* (blue branches) and SC-*Methanosarcinia* (red branches). The left heatmap presents the existence of complete C1 pathway of each type of methanogenesis. We define that the “complete C1 pathway” as: all the enzymes involving carbon substrate conversion are contained, and absent subunits ≤ 2 . The right heatmap shows the coding of cofactor enzymes involving in methanogenesis. The same heatmap presenting distribution of genes for methane-related metabolism with more detailed information is shown in Supplementary Figure 6. (b) schematic diagrams for three types of methanogenesis.



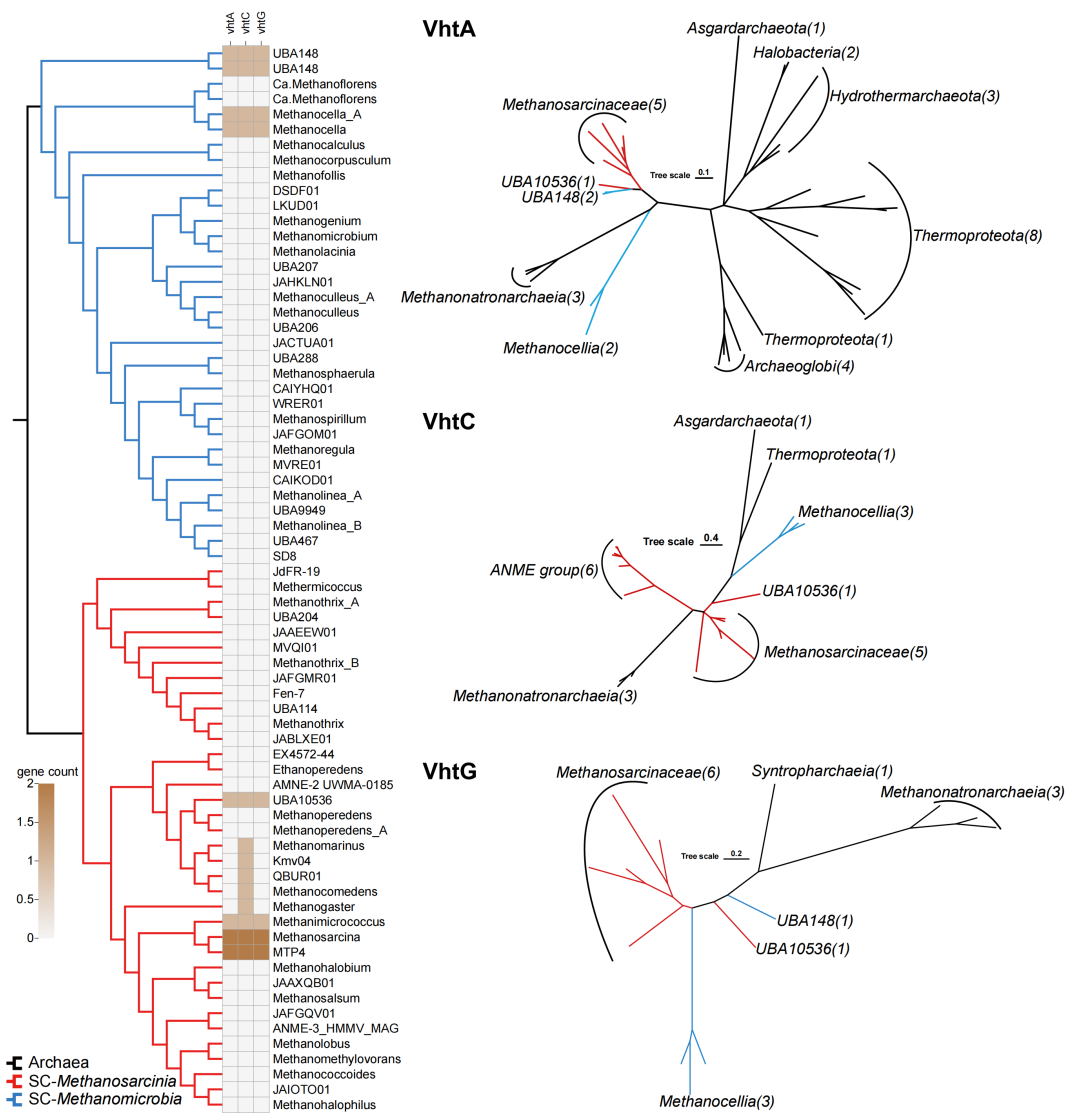
Supplementary Figure 6. The standard Gibbs free energy change when combine the hydrogenotrophic carbon dioxide reducing methanogenesis, methyl-dismutating methanogenesis and acetoclastic methanogenesis with hydrogenases-based (upper) or ETCs-based (below) energy system.



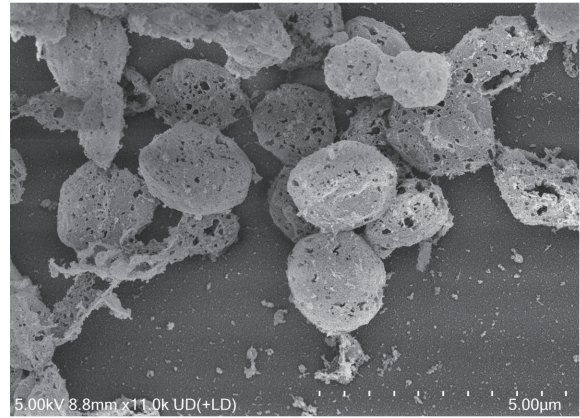
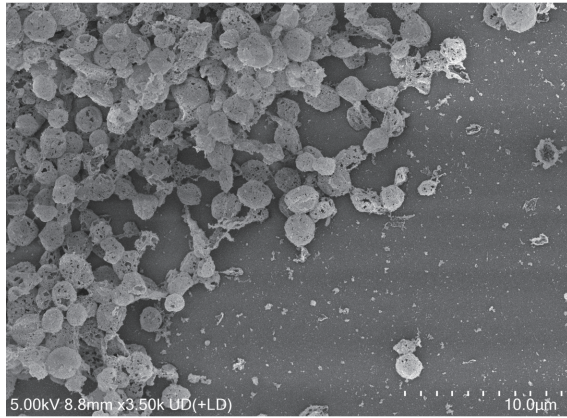
Supplementary Figure 7. The phylogenetic tree of HdrD, constructed with model LG+R8+C60 by IQ-Tree. The right table shows the coding position of HdrD as well as the co-located HdrE in the relevant genome.



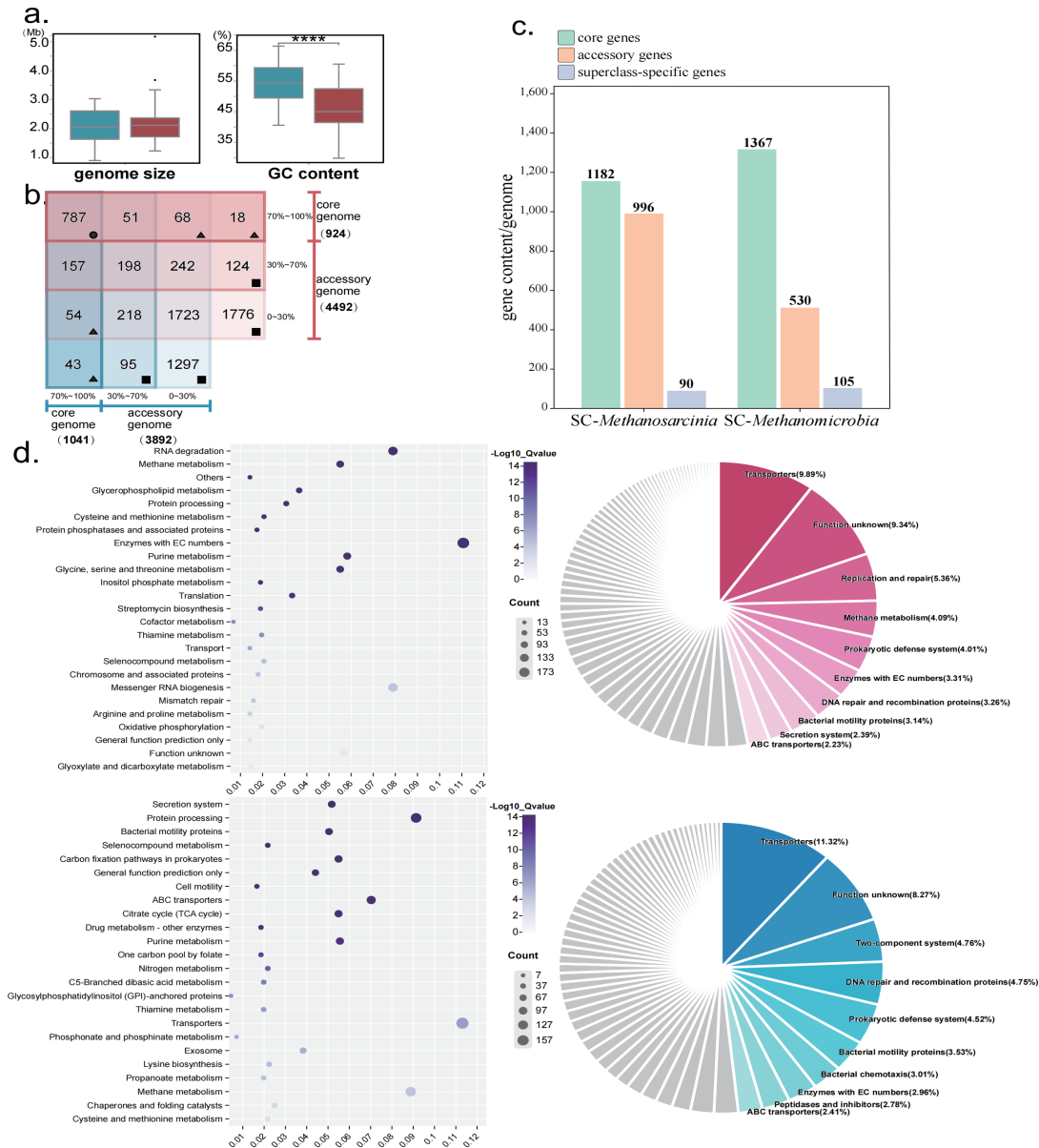
Supplementary Figure 9. Taxonomically distribution of genes coding for Fpo complex, and the phylogeny of FpoA, FpoB, FpoC, FpoD, FpoF, FpoH, FpoK, FpoL and FpoM, being constructed with the models LG+G4+C60, LG+I+G4+C60, LG+I+G4+C60, LG+R5+C60, LG+I+G4+C60, LG+F+R5+C60, LG+F+R5+C60, LG+F+I+G4+C60 and LG+F+R6+C60 by IQ-Tree, respectively. The subunits I, J, N, O are failed in acquiring homologs from GTDB archaeal and bacterial genome database, so they have no phylogenetic tree constructed here.



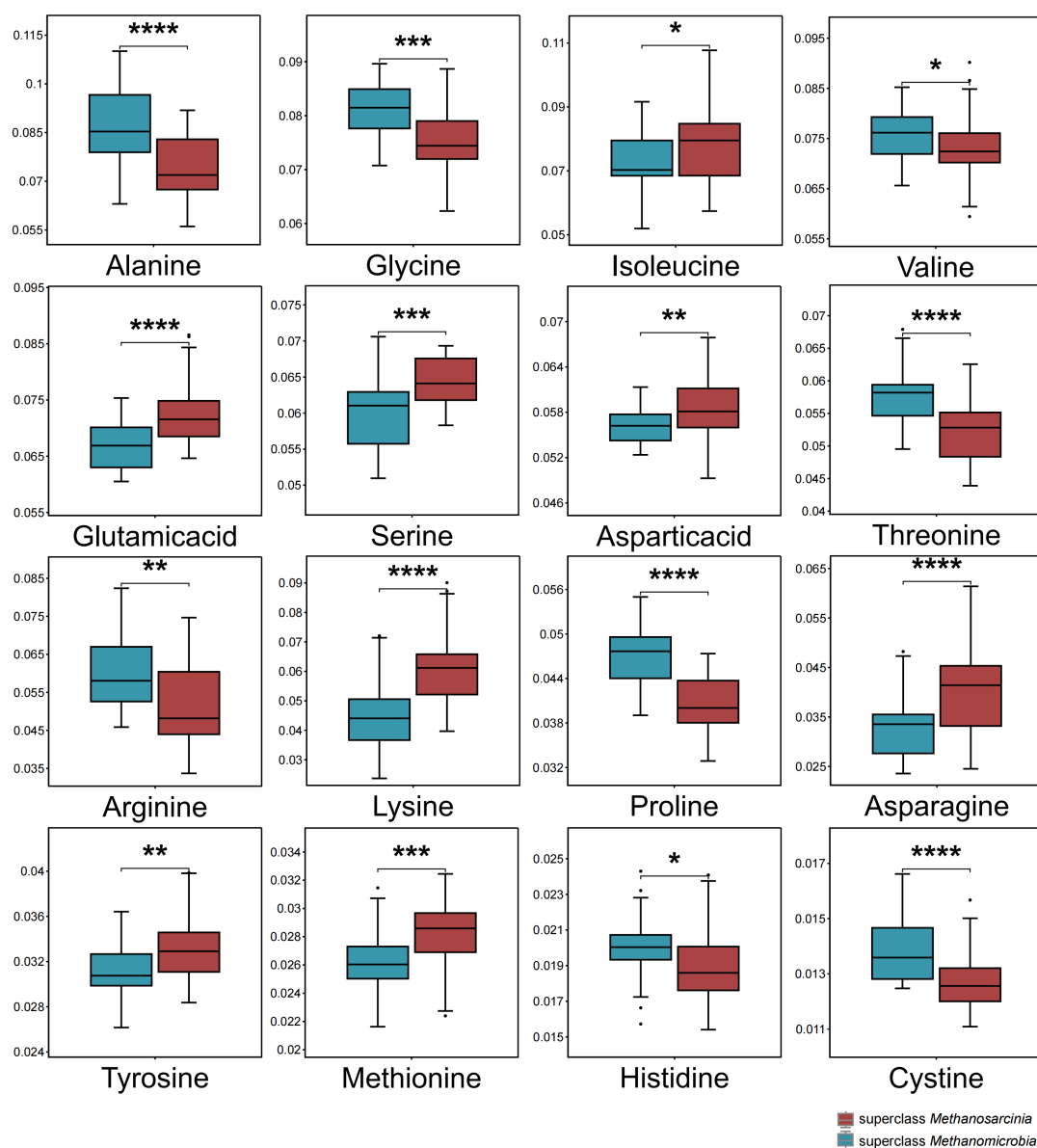
Supplementary Figure 11. Taxonomically distribution of genes coding for Vht complex, and the phylogeny of VhtA, VhtC and VhtG, being constructed with models LG+I+G4+C60, LG+I+G4+C60 and LG+I+G4+C60 by IQ-Tree, respectively.



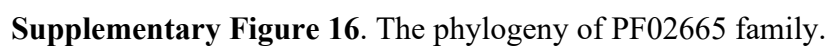
Supplementary Figure 12. Scanning electron microscopy (SEM) image of *Methanosarcina siciliae* E3.



Supplementary Figure 13. (a) Boxplots of basic information, presenting the genome size, GC content from *SC-Methanosarcinia* (n=36) and *SC-Methanomicrobia* (n=34). Stars represent the significant differences between two superclasses, determined using a Wilcoxon test (****: $p < 1e-4$). (b) Venn figure of pangenome composition. The pangenome of each superclass is divided into three parts: the orthogroups contained by >70% members, by 30~70% members and by 0~30% members. The composition of pangenome of *SC-Methanosarcinia* is represented by three red rows, and those of *SC-Methanomicrobia* is represented by three blue columns. The number in each cell refer to counts of orthogroups. (c) The average contents of core genes, accessory genes and superclass-specific genes in *SC-Methanosarcinia* and *SC-Methanomicrobia*. (d) Bubble plots of KEGG enrichment for superclass-specific genomes of *SC-Methanosarcinia* (up) and *SC-Methanomicrobia* (below), at KEGG level three category. The pie plot shows the KEGG functional composition of accessory genomes from *SC-Methanosarcinia* (up) and *SC-Methanomicrobia* (below).

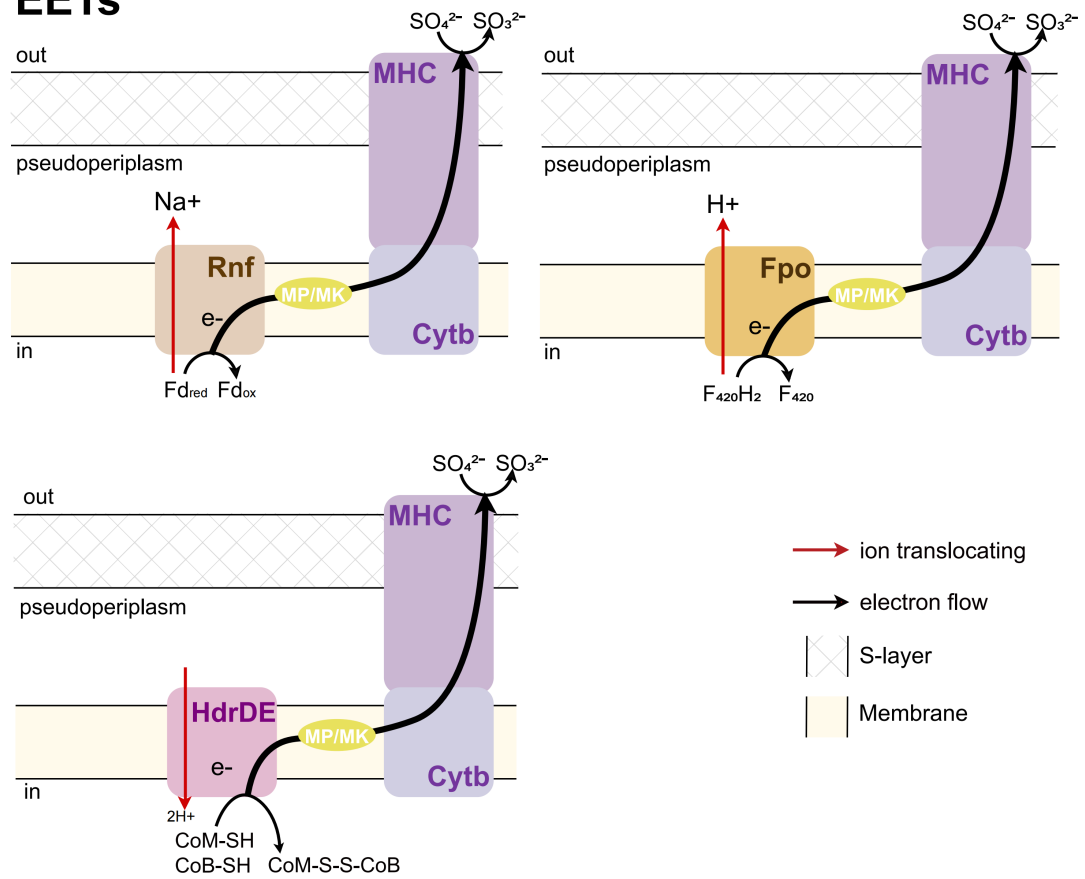


Supplementary Figure 14. Boxplots of amino acids utilization from SC-*Methanosarcinia* (n=36) (red) and SC-*Methanomicrobia* (n=34) (blue). Stars represent the significant differences between two superclasses, determined using a Wilcoxon test (****: $p < 1e-4$, ***: $p < 1e-3$, **: $p < 1e-2$, *: $p < 0.05$).

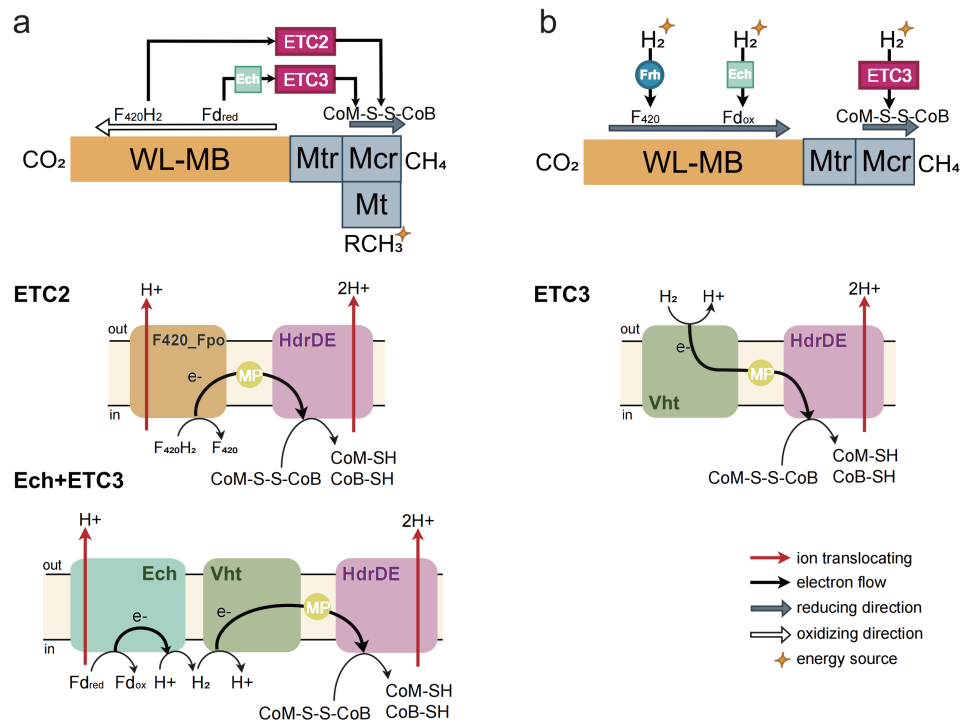


Supplementary Figure 16. The phylogeny of PF02665 family.

EETs



Supplementary Figure 17. The composition and electron transfer process of extracellular electron transfers (EETs) in ANME group from *SC-Methanosarcinia*.



Supplementary Figure 18. The electron transfer process of methyl dismutating methanogenesis (a) and carbon dioxide reducing hydrogenotrophic methanogenesis (b) in fresh water species of *Methanosarcina*.